Dual-use chromophores for photorefractive and irreversible photochromic applications

Kristi D. Harris, Rajani Ayachitula, Shane J. Strutz, L. Michael Hayden, and Robert J. Twieg

Holographic experiments are performed on a series of dual-use chromophore molecules wherein both irreversible photochromic and erasable photorefractive holographic gratings can be written in the same storage volume. At 675 nm, the chromophore undergoes a photochemical reaction leading to the creation of irreversible holographic gratings. Alternatively, at longer wavelengths, application of an electric field during grating formation allows the storage of erasable photorefractive holograms in the same location as previously stored permanent photochemical holograms. Photochemical gratings ($\eta > 60\%$) can be written in less than 1 min, whereas photorefractive gratings ($\eta > 50\%$) can be written in less than 1 s. The photochemical gratings have a diffusion-limited dark half-life of as long as two weeks depending on the glass transition temperature of the composite. © 2001 Optical Society of America

OCIS codes: 050.7330, 100.0100, 160.2900, 160.5320, 160.5470.

1. Introduction

Photorefractive (PR) polymers are potential replacements for PR crystals. The rapid response times and high diffraction efficiency[1–3] of these polymers, combined with their low cost, have led to their study for various real-time holographic applications such as phase conjugation,[4] imaging through distorting media,[5] digital data storage,[6] the coupling of light into waveguides,[7] and ultrasound detection.[8]

A subset of the many types of inorganic PR crystal, $Bi_{12}SiO_{20}$,[9,10] $Bi_{12}TiO_{20}$,[11] and semiconductors such as GaP[12] have already been shown to exhibit a dual-grating behavior. In these materials, photochromic (PC) gratings are formed during the PR grating formation process. These dual-grating materials are useful for applications that benefit from the interaction between light diffracted from two simultaneous gratings. These applications[13] include wave-front interferometry, image synthesis, logic operations, phase object detection, holographic interferometry, and novel spatial light modulation.

Here we present results on polymer composites capable of simultaneously storing both erasable PR and irreversible PC holograms. Although the PC reaction is irreversible, the lifetime of the gratings formed by that reaction depends on the composite's glass transition temperature, which affects the translational diffusion of the photochemically altered chromophores. Gratings can be formed in the following combinations: PC only (at 675 nm with no external field), PC and PR simultaneously (at 675 nm under the application of an external field), or PR only (at wavelengths longer than 715 nm with an applied field). The different response times of the PR and PC effects could make dual-use materials useful in the creation of an optical tracking novelty filter with a broad range of detectable velocities.[14]

2. Experimental Details

Our composites consist of the photoconductor poly(*N*-vinyl carbazole) (PVK), the plasticizers butyl benzyl phthalate (BBP) or tricresyl phosphate (TCP), the sensitizer and charge generators of fullerene C_{60} or 2,4,7-trinitro-9-fluorenone (TNF), and a series of chromophores with differing modifications of the benzene ring of [2-(5,5-dimethyl-3-styr-cyclohex-2-enylidene)-malononitrile] (DCPT). These chromophores (Fig. 1) perform two functions in our composites. First, they are chromophores with large PR molecular figures of merit (FOM),[15]

K. D. Harris, R. Ayachitula, S. J. Strutz, and L. M. Hayden (hayden@umbc.edu) are with the Department of Physics, University of Maryland, Baltimore County, 1000 Hilltop Circle, Baltimore, Maryland 21250-0000. R. J. Twieg is with the Department of Chemistry, Kent State University, Kent, Ohio 44242.

4NEt2DCPT **4NPh2DCPT** **3NEtCarb**
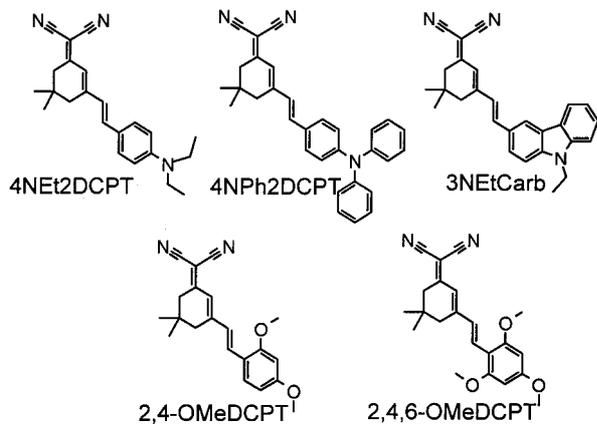
2,4-OMeDCPT **2,4,6-OMeDCPT**

Fig. 1. Chromophore structures.

allowing the formation of efficient PR gratings. Second, these chromophores are photochemically active, possibly by 2 + 2 photochemical reactions, especially when triplet sensitized.[16] These photochemical reactions can be used to write irreversible PC gratings.

Previously, we investigated the chromophore (3-(2-(4-(N,N-diethylamino)phenyl)ethenyl)-5,5-dimethyl-1,2-cyclohexenylidene)-propanedinitrile (Lemke, denoted here as 4NEt2DCPT).[17] In that study we investigated composites of PVK:4NEt2DCPT:BBP:C$_{60}$ at 72–56:7:21–36:1 wt.% and found them to be efficient materials for storing both PR and PC gratings. We demonstrated the multiplexing of ten PC gratings and one PR grating in the same storage volume simultaneously. In the research presented here we focus on increasing the dye concentration in our polymer composites by using dyes with lower absorption at 675 nm.

Figure 2 shows the UV–visible spectra of the chromophores in dichloromethane (DCM). We found the molecules 4NPh2DCPT, 3NEtCarb, 2,4,6-OMeDCPT, and 2,4-OMeDCPT to have absorption peaks of 493,
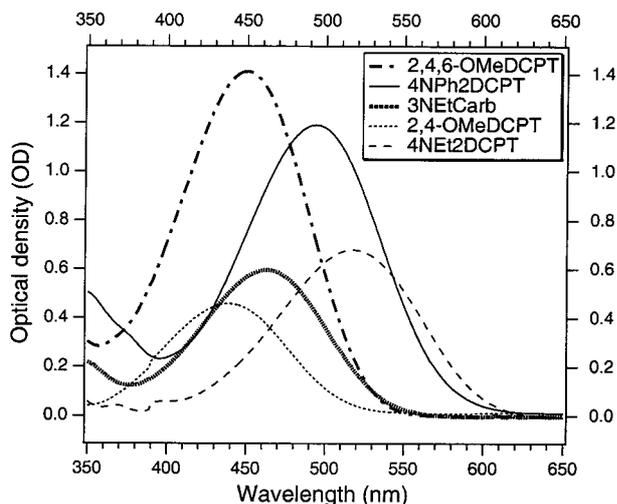
4NEt2DCPT has a peak absorption at 517 nm. These changes in absorption generally reflect the changes in donor capability of substituents on the benzene ring of the parent DCPT. On the basis of these results, we believed it possible to incorporate at least twice as much dye into our polymer composites as was used in the previous 4NEt2DCPT system and still maintain a reasonable transmission at the writing wavelength of 675 nm. These chromophores were all prepared in a straightforward fashion by condensation of 3-dicyanomethylidene-1,5,5-trimethylcyclohex-1-ene with the appropriate aromatic aldehyde. For example, the preparation of 4NEt2DCPT is already described by Lemke.[18] The preparation of the chromophore 4NPh2DCPT (and a number of related electro-optical chromophores) is also described in detail.[19] The synthesis of 4NPh2DCPT and two similar molecules was also recently reported.[20]

We purified the polymer PVK (Aldrich; average M_w at approximately 1,100,000) through precipitation by dripping its 10-wt.% DCM solution in either methanol (while stirring) or boiling ethanol. We purified the plasticizer TCP (Aldrich; a mixture of isomers) by boiling it with activated carbon for 4 h and by using column chromatography over natural silica gel with THF (tetrahydrofuran) as the eluent. The plasticizer BBP (Scientific Polymer Products) and the sensitizers C$_{60}$ (Aldrich) and TNF (Pfaltz & Bauer) were used as received. We determined the T_g of each composite by monitoring the second-harmonic generation from 10-μm-thick films that were appropriately dried and corona poled.[21] We made the PR–PC films by casting them from solvent and filtering them through a 0.2-μm Teflon or glass–nylon filter. From the evaporated material, we fabricated films approximately 75 μm thick by heating the solid ($T = 150–180$ °C) while pressing the films between two glass slides. Kapton spacers were used to produce polymer films of uniform thickness. The constituents and the T_g of each composite are given in Tables 1 and 2.

Degenerate four-wave mixing was used to write and monitor the holographic gratings in each composite. The separation angle between the two write beams was 22°; for the PR measurements, the sample normal was tilted at an angle of 60° from the bisector of the two write beams. Samples used to study the PR effect were prepared between two glass slides coated with indium tin oxide. PR experiments were performed with either a Ti:sapphire laser, tunable between 715 and 820 nm, or a 675-nm laser diode. To observe only the PR effect at 675 nm, the writing times were limited to only a few seconds. By limiting the total writing time per sample, we were able to prevent the formation of PC gratings. For verification, we continued to monitor the diffracted signal after removal of the electric field to ensure the diffracted signal's return to background level. Because of the higher PC sensitivity of the 4NPh2DCPT–2,4-OMeDCPT composite, we were unable to write PR

Fig. 2. UV–visible spectra of the chromophores in DCM.

Table 1. Photorefractive Results and Experimental Details

Symbols used in Fig. 3	Composition[a]	T_g (°C)	λ (nm)	η_{ext}[b] (%)	I_{write} (W/cm^2)	d_{film} (μm)
○	3NEtCarb (15%), TCP (35%), C$_{60}$ (1%)	32	675	28	1.6	75
▲	3NEtCarb (15%), BBP (36%), TNF (1%)	29	675	12	0.1	78
◆	4NEt2DCPT (7%), BBP (36%), C$_{60}$ (1%)	26	675	12	0.2	75
■	4NEt2DCPT (7%), BBP (24%), C$_{60}$ (1%)	67	730	10	0.2	156
△	4NPh2DCPT (15%), BBP (32%), C$_{60}$ (1%)	58	730	9	0.2	75
●	2,4-OMeDCPT (15%), BBP (23%), C$_{60}$ (1%)	70	730	2	0.2	75
✱[c]	2,4,6-OMeDCPT (5%), BBP (24%), C$_{60}$ (1%)	59	675	1	1.6	103
✱[c]	4NEt2DCPT (7%), BBP (24%), C$_{60}$ (1%)	67	675	1	0.2	75
▼	4NPh2DCPT (18%), BBP (24%), C$_{60}$ (1%)	70	730	0.1	0.2	75

[a]Remaining percentage to 100% is PVK.
[b]η_{ext} is the maximum external diffraction efficiency attained.
[c]Denotes data not plotted.

gratings at 675 nm without the attendant formation of small PC gratings, even for short exposure times.

We also probed the PC grating formation using a degenerate four-wave mixing configuration. For these experiments, the polymer was pressed between plain glass slides with the sample normal bisecting the two write beams. A 675-nm laser diode was used to generate the coherent s-polarized write beams ($\approx$1.8 W/cm^2) and the p-polarized read beam (0.05 W/cm^2).

3. Results and Discussion

The PR external diffraction efficiency η_{ext} plotted in Fig. 3 is the ratio of the diffracted intensity to the incident intensity. Of the low-T_g materials [Fig. 3(a)], a maximum η_{ext} of 28% was attained with the (15%) 3NEtCarb–TCP–C$_{60}$ composite, an improvement from the maximum η_{ext} of 11.5% achieved with the (7%) 4NEt2DCPT system with a similar T_g and an identical sensitizer. Although both samples exhibited 100% internal diffraction efficiency, with 4NEt2DCPT showing a maximum at an applied field of 80 V/μm and 3NEtCarb at 95 V/μm, the higher η_{ext} can be explained by the reduced absorption and higher concentration of the 3NEtCarb chromophore as compared with the 4NEt2DCPT. Molecular orbital calculations predict a higher molecular FOM for 4NEt2DCPT as compared with 3NEtCarb, a fact that is confirmed when we compare the peak in the η_{ext}

versus the field for the two systems. By comparing the location of the peak in η_{ext} for the two 3NEtCarb curves in Fig. 3(a), we can also assert that changing the sensitizer from TNF to C$_{60}$ results in a more efficient response at 675 nm (compare the filled triangles with the open circles). A final comment relates to the effect of changing the plasticizer from BBP to TCP in the 3NEtCarb composites. Microscopic examination of the 3NEtCarb–BBP samples revealed two phases that were evenly distributed across the film. The result is that for a given illumination area; there were fewer dye molecules in the phase-separated samples, which resulted in a lower overall diffraction efficiency (compare the filled triangles with the open circles).

As shown in Fig. 3(b), not only are the high-T_g materials less efficient at writing PR gratings, but neither the 4NPh2DCPT nor the 2,4-OMeDCPT systems compare favorably with the original 4NEt2DCPT system with a similar T_g. Only when we decrease the T_g to 58 °C does the (15%) 4NPh2DCPT system approach the (7%) 4NEt2DCPT results. This is an indication of the sensitivity of the chromophore mobility on the local polymer environment. A shift of only 12 °C in the T_g makes a dramatic difference in the response (compare the inverted filled triangles with the open triangles). We also performed semiempirical calculations (AM1, PRECISE, and EF in MOPAC6) on these molecules to

**Table 2. Photochromic Results and Experimental Details[a]**

Symbols used in Fig. 4	Composition[b]	T_g (°C)	S (cm^2/J)	I_{write} (W/cm^2)	d_{film} (μm)
□	4NPh2DCPT (15%), 2,4-OMeDCPT (15%), BBP (25%), C$_{60}$ (1%)	32	3.7×10^{-3}	1.8	75
▼	4NPh2DCPT (18%), BBP (24%), C$_{60}$ (1%)	70	2.3×10^{-3}	1.8	75
△	4NPh2DCPT (15%), BBP (32%), C$_{60}$ (1%)	58	1.9×10^{-3}	1.8	75
○	3NEtCarb (15%), TCP (35%), C$_{60}$ (1%)	32	1.8×10^{-3}	1.8	75
◆	4NEt2DCPT (7%), BBP (36%), C$_{60}$ (1%)	26	1.7×10^{-3}	1.8	75
●	2,4-OMeDCPT (15%), BBP (23%), C$_{60}$ (1%)	70	1.4×10^{-3}	1.8	75
◇	2,4,6-OMeDCPT (5%), BBP (24%), C$_{60}$ (1%)	59	1.4×10^{-3}	1.6	92
■	4NEt2DCPT (7%), BBP (24%), C$_{60}$ (1%)	67	0.5×10^{-3}	1.8	75

[a]All PC experiments were performed at 675 nm.
[b]Remaining percentage to 100% is PVK.
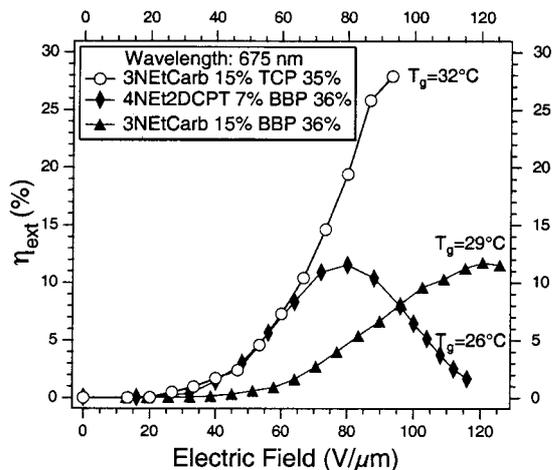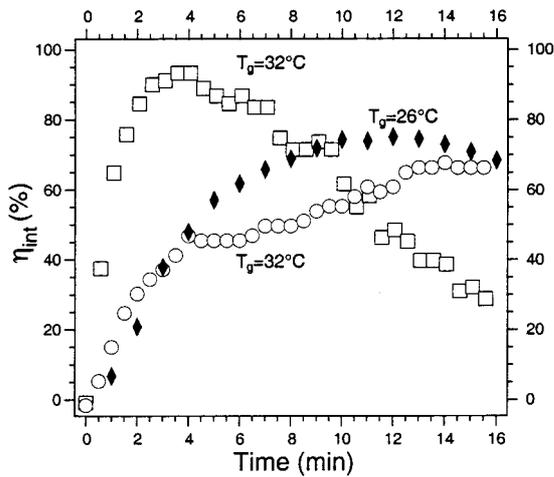
(a)
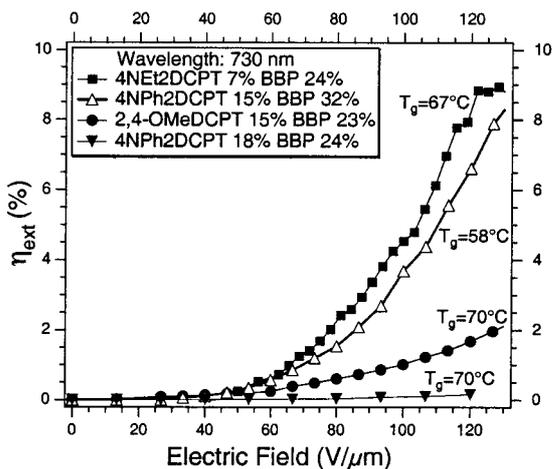
(b)

Fig. 3. Photorefractive external diffraction efficiency η_{ext} as a function of the applied field for the (a) low-T_g composites and (b) the high-T_g composites. Data symbols correspond to those in Table 1. All composites contain 1-wt.% C_{60} as a sensitizer except for the composite 3NEtCarb (15%) and BBP (36%) in (a), which contains 1-wt.% TNF. The remaining percentage to 100% is PVK in all composites.

obtain the ground-state dipole moment μ, the anisotropy of the linear polarizability $\Delta\alpha$, and the first hyperpolarizability β to further aid in the explanation of these results. Scaling each parameter to the 4NEt2DCPT value, we calculated the following values for the three chromophores 4NEt2DCPT, 2,4-OMeDCPT, and 4NPh2DCPT: μ(1:0.9:0.8), $\Delta\alpha$(1:1: 0.8), β(1:1:0.6). The PR FOM scales with $\mu^2\Delta\alpha$. The first hyperpolarizability β also affects the FOM but to much less of a degree when orientational enhancement[22] is present. To account for the molar volume of the chromophores, we divide the FOM by the molar mass[23] to obtain the relative FOM's (1:0.8:

0.5) for these three composites, respectively. Figure 3(b) shows that, even after we account for the differences in chromophore concentration and the relative FOM's, 4NEt2DCPT is substantially better than the other two molecules. This result suggests that the shape of the chromophore and hence its interaction with the polymer host may also affect the degree of orientational enhancement. We also note that when the T_g of the 4NPh2DCPT composite is decreased to 58 °C, allowing orientational enhancement to occur, the diffraction efficiency of 4NPh2DCPT (open triangles) is similar to that for 4NEt2DCPT (filled squares). This result is in good agreement with the prediction from the molecular orbital calculations after we account for the chromophore concentration. The details of the PR experiments on all these DCPT derivatives are summarized in Table 1.

The PC internal diffraction efficiency η_{int} plotted in Fig. 4 is the ratio of the diffracted intensity to the intensity transmitted through the sample before the grating was written. The initial slopes of the curves in Fig. 4 yield the sensitivities S of the different composites, defined here as the square root of the diffraction efficiency divided by the exposure. The sensitivities are higher for the lower-T_g composites because the photochemical grating formation depends on the translational diffusion of the combining chromophores, as discussed earlier.[17] Higher sensitivities have been obtained in a similar material by use of shorter wavelengths, higher concentrations, and alternative sensitizers.[24] The details and results of the PC experiments are summarized in Table 2.

When we compare the high-T_g PR and PC results [Fig. 3(b) and 4(b)], an apparent contradiction in the 4NEt2DCPT (filled squares) and 4NPh2DCPT (inverted filled triangles) results is evident in that, for the PC case, the 4NPh2DCPT (inverted filled triangles) composite is more efficient and more sensitive than the 4NEt2DCPT (filled squares) composite, whereas the 4NEt2DCPT (filled squares) composite is more efficient in the PR case. We believe there are two contributing causes for this effect. First, the diffraction efficiency and sensitivity are expected to scale superlinearly with concentration because the PC reaction is governed by the transfer of triplet energy from the C_{60} sensitizer to the chromophores by a process that depends on the exponential overlap of their wave functions. In addition, the rate of the PC reaction between two triplet-sensitized chromophores is proportional to the product of their concentrations. The combined effect of these features of the PC reaction leads to a superlinear dependency of the PC diffraction efficiency on concentration. Second, studies of the translation–rotation paradox by Hall et al.[25] showed that orientational rotation times and translational diffusion times near T_g are different, with rotational times being much longer. They report that near T_g a dopant can translate (by diffusion) over 70 times its length during the average orientational rotation time. They also report that this enhancement of translation relative to rotation

(a)
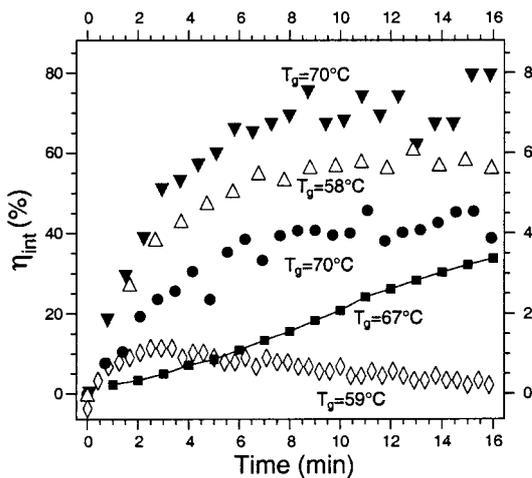
(b)

Fig. 4. Photochemical internal diffraction efficiency η_{int} at 675 nm as a function of writing time for (a) the low-T_g composites and (b) the high-T_g composites. Data symbols correspond to those in Table 2. Chromophore and plasticizer content for graph (a): open square, 4NPh2DCPT (15%), 2,4-OMeDCPT (15%), BBP (25%); filled diamond, 4NEt2DCPT (7%), BBP (36%); open circle, 3NEtCarb (15%), TCP (35%). Graph (b): inverted filled triangle, 4NPh2DCPT (18%), BBP (24%); open triangle, 4NPh2DCPT (15%), BBP (32%); filled circle, 2,4-OMeDCPT (15%), BBP (23%); filled square, 4NEt2DCPT (7%), BBP (24%); open diamond, 2,4,6-OMeDCPT (5%), BBP (24%). In all composites, the sensitizer is 1-wt.% C_{60}, and the remaining percentage to 100% is PVK.

will be present at other temperatures provided that the distribution of relaxation times is temperature dependent. We measured this effect (see discussion below) and found that the distribution parameter β varies from 1 to 0.5 over the temperature range studied. In particular, in the glassy state we found (Fig. 6) that β = 0.7 (T_g = 67 °C) and β = 0.5 (T_g = 108 °C). This implies that dopants will experience enhanced translation relative to rotation. This explains the apparent discrepancy between our PR (rotation-
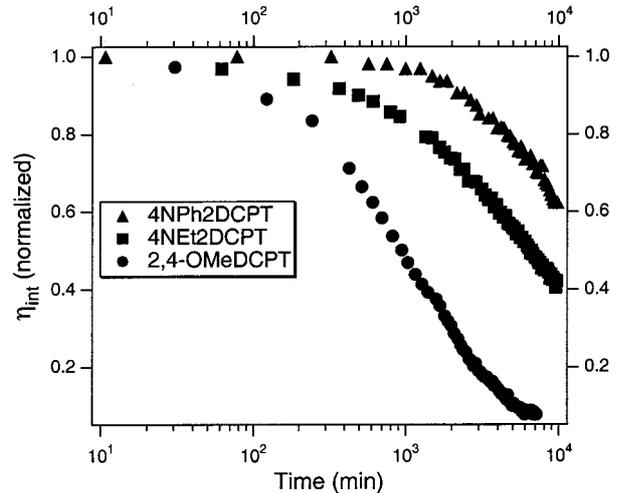

Fig. 5. Effect of chromophore size and structure on the dark decay of photochemical gratings in three composites with T_g = 67 °C.

dependent) and PC (translation-dependent) results for 4NEt2DCPT (filled squares) and 4NPh2DCPT (inverted filled triangles).

A maximum η_{int} of 94% was reached in the low-T_g material (15%) 4NPh2DCPT–(15%) 2,4-OMeDCPT. The decrease in η_{int} after reaching a maximum value in the low-T_g systems is due not to overmodulation but to the translational diffusion of the molecules that formed the grating. Thus, after a grating is formed, translational diffusion of reacted and unreacted chromophores causes the grating contrast to diminish in low-T_g systems. Translational diffusion also affects the dark storage time of the gratings. Figure 5 shows the dark decay in three different composites with the same T_g = 67 °C probed periodically with a weak reading beam at 675 nm. The relative decay times scale with the size of the donors in the chromophores; the bulkier chromophores give rise to longer decay times.

We also studied the effect of the T_g of the composite on the dark decay times of the PC gratings (Fig. 6). For this test, we wrote a grating to its maximum efficiency (~20% externally) and periodically read the grating with a 0.05-W/cm^2 beam for 5 s every 2 min for the low-T_g composites (26 and 38 °C) and for 1 min every hour for the higher-T_g systems. The short exposure times minimized the grating decay during readout. For example, continuous reading of the 108 °C composite for 2 h at this exposure reduced the square root of the diffraction efficiency by only 3%.

We fit the decays in Fig. 6 to a Kohlrausch–Williams–Watts stretched exponential function,[26]

$$\sqrt{\eta(t)} = \sqrt{\eta(0)} \, \exp[-(t/\tau)^\beta], \qquad (1)$$

where η is the diffraction efficiency, τ is the characteristic decay time, and β reflects the width of the distribution of decay times and ranges from zero to one. The nonexponential nature of the decay can be interpreted as a superposition of diffusion events in a heterogeneous environment giving rise to a distribu-
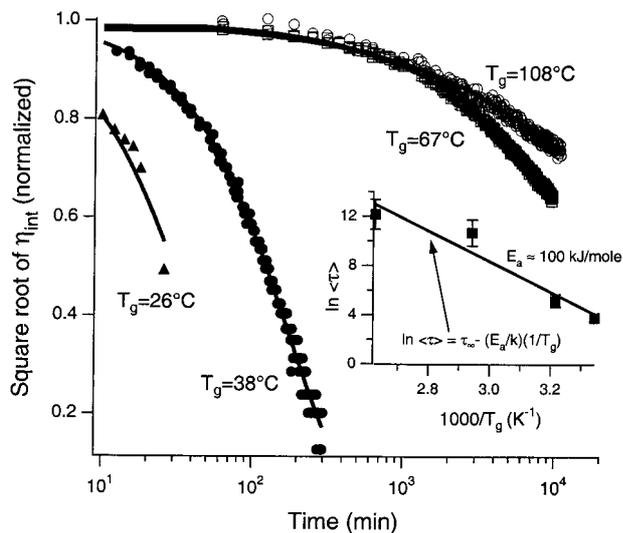
Fig. 6. Effect of the glass transition temperature on the dark decay times in composites based on (7%) 4NEt2DCPT. Inset is an Arrhenius plot of grating decay times.

tion of times associated with any individual diffusion. Such a distribution suggests that we use an average value for the times,[27]

$$\langle \tau \rangle = \int_0^\infty \exp\left[-\left(\frac{t}{\tau}\right)^\beta \right] dt = \frac{\tau \Gamma(1/\beta)}{\beta}, \qquad (2)$$

where Γ is the gamma function. The Kohlrausch–Williams–Watts function is widely used to model relaxations in polymers.[25,28] In the inset to Fig. 6, we show an Arrhenius fit to the grating decay data with an apparent activation energy $E_a = 100$ kJ/mol. Relaxations in polymers that involve long-range cooperative motion, such as the α relaxation associated with the glass transition, typically have activation energies of 200–400 kJ/mol, whereas relaxations associated with smaller units (β and γ transitions, etc.) have activation energies ranging from 10 to 100 kJ/mol.[29] In addition, diffusion of small molecules (water, for example) in polymers have activation energies in the 60-kJ/mol range.[29] Therefore, because we interpret the 100-kJ/mol activation energy associated with the dark decay of the PC gratings to be the result of the diffusion of chromophores, the diffusion of these molecules is apparently facilitated by a relaxation in PVK that is similar to secondary relaxations in other polymeric materials. Unfortunately, we could find no reports of dielectric or mechanical relaxation measurements in PVK with which to compare our results. However, if our supposition is correct, then a clear way to increase the grating dark lifetime would be to covalently attach some of the chromophores to the polymer backbone, thereby coupling the chromophore diffusion to the motions of the polymer backbone. This arrangement would likely raise the activation energy for grating decay to the 200–400-kJ/mol range associated with long-range

motion seen in most polymers and hence extend the dark lifetime.

4. Conclusions

The main advantage of our composites is that they are capable of storing both erasable and irreversible holograms in the same storage volume.[17] In addition, the grating formation processes are wavelength selective, allowing for the formation of simultaneous PR and PC gratings or each grating type individually. Use of 675-nm light and an external electric field causes the formation of both grating types (on different time scales), allowing applications such as holographic interferometry, image synthesis, and logic operations to be implemented. When longer wavelengths (>730 nm) are used, purely PR holographic operations such as optical switching and imaging through distorting media are possible. Van Steenwinckel et al.[20] recently reported PR results with 4NPh2DCPT at 780 nm with (2,4,7-trinitro-9-fluorenylidene)malononitrile (TNFDM). We did not observe any PC gratings in any of the materials studied here at any wavelength (675–820 nm) when we used TNF or TNFDM as a sensitizer.

Clearly, further enhancements in the materials' properties will be required. Some simple modifications in the structures of the DCPT derivatives to render them less prone to crystallization and phase separation are planned. Likewise, other plasticizers and the issues of purity of all the components in the mixtures need to be examined. With such enhancements of the materials, long-term storage applications such as digital data storage may be possible by the writing of purely PC gratings at 675 nm with no external field. We have shown that the writing times in the PC materials scale with the number of chromophores and are inversely proportional to the T_g. In addition, the dark decay times appear to be dependent on the translational diffusion of the chromophores. We are currently working on some of the applications noted above and will report those results elsewhere.

References

1. K. Meerholz, B. L. Volodin, Sandalphon, B. Kippelen, and N. Peyghambarian, "A photorefractive polymer with high optical gain and diffraction efficiency near 100%," Nature (London) **371,** 497–500 (1994).
2. M. A. Diaz-Garcia, D. Wright, J. D. Casperson, B. Smith, E. Glazer, W. E. Moerner, L. I. Sukhomlinova, and R. J. Twieg, "Photorefractive properties of poly(N-vinyl carbazole)-based composites for high-speed applications," Chem. Mater. **11,** 1784–1791 (1999).
3. F. Würthner, R. Wortmann, R. Matschiner, K. Lukaszuk, K. Meerholz, Y. DeNardin, R. Bittner, C. Bräuchle, and R. Sens,

"Merocyanine dyes in the cyanine limit: a new class of chromophores for photorefractive materials," Agnew. Chem. Int. Ed. Engl. **36,** 2765–2768 (1997).

4. A. Grunnet-Jepsen, C. L. Thompson, and W. E. Moerner, "Spontaneous oscillation and self-pumped phase conjugation in a photorefractive polymer optical amplifier," Science **277,** 549–552 (1997).

5. B. Kippelen, S. R. Marder, E. Hendrickx, J. L. Maldonado, G. Guillemet, B. L. Volodin, D. D. Steele, Y. Enami, Sandalphon, Y. J. Yao, J. F. Wang, H. Röckel, L. Erskine, and N. Peyghambarian, "Infrared photorefractive polymers and their applications for imaging," Science **279,** 54–57 (1998).

6. P. M. Lundquist, C. Poga, R. G. DeVoe, Y. Jia, W. E. Moerner, M.-P. Bernal, H. Coufal, R. K. Grygier, J. A. Hoffnagle, C. M. Jefferson, R. M. Macfarlane, R. M. Shelby, and G. T. Sincerbox, "Holographic digital data storage in a photorefractive polymer," Opt. Lett. **21,** 890–892 (1996).

7. D. Kokron, S. M. Evanko, and L. M. Hayden, "Launching of guided waves in a photorefractive polymer by two-beam coupling," Opt. Lett. **20,** 2297–2299 (1995).

8. M. B. Klein, G. D. Bacher, A. Grunnet-Jepsen, D. Wright, and W. E. Moerner, "Homodyne detection of ultrasonic surface displacements using two-wave mixing in photorefractive polymers," Opt. Commun. **162,** 79–84 (1999).

9. P. M. Jeffrey, S. L. Clapham, R. W. Eason, D. A. Eason, D. A. Fish, A. K. Powell, T. J. Hall, and N. A. Vainos, "Mechanism of photorefractive enhancement of photochromic gratings in BSO-experimental results and phenomenological modelling," Opt. Commun. **98,** 357–365 (1993).

10. D. A. Fish, A. K. Powell, T. J. Hall, P. M. Jeffrey, and R. W. Eason, "Theoretical analysis of mechanism of photorefractive enhancement of photochromic gratings in BSO," Opt. Commun. **98,** 349–356 (1993).

11. J. Frejlich and P. M. Garcia, "Quasipermanent hole-photorefractive and photochromic effects in $Bi_{12}TiO_{20}$ crystals," Appl. Phys. A **55,** 49–54 (1992).

12. K. Horiuchi and K. Kuroda, "Photorefractive and photochromic effects in undoped GaP at high temperature," Opt. Commun. **113,** 487–492 (1995).

13. N. A. Vainos, S. L. Clapham, and R. W. Eason, "Applications of multiplexed real time and permanent holographic recording in photorefractive BSO," Appl. Opt. **28,** 4386–4392 (1989).

14. A. Chen, S. Fan, H. Ding, and C. Wu, "Extension of the velocity detection range of a tracking novelty filter that uses $LiNbO_3$ and strontium barium niobate," Appl. Opt. **33,** 2998–3002 (1994).

15. S. R. Marder, B. Kippelen, A. K.-Y. Jen, and N. Peyghambarian, "Design and synthesis of chromophores and polymers for electro-optic and photorefractive applications," Nature (London) **388,** 845–851 (1997).

16. R. Wortmann, P. M. Lundquist, R. J. Twieg, C. Geletneky, C. R. Moylan, Y. Jia, R. G. DeVoe, D. M. Burland, M.-P. Bernal, H. Coufal, R. K. Grygier, J. A. Hoffnagle, C. M. Jefferson, R. M. Macfarlane, R. M. Shelby, and G. T. Sincerbox, "A novel sensitized photochromic organic glass for holographic optical storage," Appl. Phys. Lett. **69,** 1657–1659 (1996).

17. S. J. Strutz and L. M. Hayden, "Quasipermanent photochemical gratings in a dual use photorefractive polymer composite," Appl. Phys. Lett. **74,** 2749–2751 (1999).

18. R. Lemke, "Solvatochromiie von 80 mμ in verschiedenen Alkoholen bei Arylidenisophoron-Abkommlingen," Chem. Ber. **103,** 1894–1895 (1970).

19. S. Ermer, S. M. Lovejoy, D. S. Leung, H. Warren, C. R. Moylan, and R. J. Twieg, "Synthesis and nonlinearity of triene chromophores containing the cyclohexene ring structure," Chem. Mater. **9,** 1437–1442 (1997).

20. D. Van Steenwinckel, E. Hendrickx, A. Persoons, K. Van den Broeck, and C. Samyn, "Influence of the chromophore ionization potential on speed and magnitude of photorefractive effects in poly(N-vinylcarbazole) based polymer composites," J. Chem. Phys. **112,** 11030–11037 (2000).

21. L. M. Hayden, S. C. Brower, and S. J. Strutz, "Pressure dependence of the depoling temperature in nonlinear optical polymers," Macromolecules **30,** 2734–2737 (1997).

22. W. E. Moerner, S. M. Silence, F. Hache, and G. C. Bjorklund, "Orientationally enhanced photorefractive effect in polymers," J. Opt. Soc. Am. B **11,** 320–330 (1994).

23. R. Wortmann, C. Glania, P. Krämer, K. Lukaszuk, R. Matschiner, R. J. Twieg, and F. You, "Highly transparent and birefringent chromophores for organic photorefractive materials," Chem. Phys. **245,** 107–120 (1999).

24. A. Akella, S. L. Sochava, and L. Hesselink, "Synthesis and characterization of photochromic organic films for holographic recording," Opt. Lett. **22,** 919–921 (1997).

25. D. B. Hall, A. Dhinojwala, and J. M. Torkelson, "Translation-rotation paradox for diffusion in glass-forming polymers: the role of the temperature dependence of the relaxation time distribution," Phys. Rev. Lett. **79,** 103–106 (1997).

26. G. Williams and D. C. Watts, "Non-symmetrical dielectric relaxation behaviour arising from a simple empirical decay function," Trans. Faraday Soc. **66,** 80–85 (1970).

27. C. P. Lindsey and G. D. Patterson, "Detailed comparison of the Williams-Watts and Cole-Davidson functions," J. Chem. Phys. **73,** 3348–3357 (1980).

28. M. T. Cicerone, P. A. Wagner, and M. D. Ediger, "Translational diffusion on heterogeneous lattices: a model for dynamics in glass forming materials," J. Phys. Chem. B **101,** 8727–8734 (1997).

29. N. E. McCrum, B. E. Read, and G. Williams, *Anelastic and Dielectric Effects in Polymeric Solids* (Dover, New York, 1967).